Struct Chem (2016) 27:295–303
DOI 10.1007/s11224-015-0700-y

ORIGINAL RESEARCH

Synthesis and spatial structure of new chiral dopants from allobetuline series for cholesteric liquid-crystal compositions

Nikolay L. Babak[1] · Oleg V. Shishkin[1,2] · Svitlana V. Shishkina[1,3] · Ivan M. Gella[1,3] · Vladimir I. Musatov[1] · Nataliya B. Novikova[1] · Victoria V. Lipson[1,2,3]

Received: 4 November 2015 / Accepted: 6 November 2015 / Published online: 20 November 2015

Abstract New series of chiral dopants for cholesteric liquid-crystal compositions were synthesized on the base of 2-substituted allobetuline derivatives, and their steric structure was determined by X-ray analysis. The relationship between spatial structure of these compounds and their ability to induce cholesteric helix in 4-pentyl-4′-cyanobiphenyl nematic solvent was examined. The highest values of the helical twisting power $|\beta|$ (71.38 ± 3.4) and (84.25 ± 3.7) mkm^{-1} $mol{\cdot}pats^{-1}$ showed (*E*)-2-(4-chlorophenylmethylidene)-allobetuline and (2*R*,3*R*)-3-(4′-chlorophenyl)-2,2′-spiro-oxyranoallobetuline correspondingly. How the value of $|\beta|$ in this series of compounds varies depending on the spatial arrangement relative to the aryl moiety of the chiral core is shown.

Keywords Allobetuline derivatives · Chiral dopants for cholesteric liquid-crystal compositions · Helical twisting power · Molecular structure · Quantum-chemical calculations

Introduction

Liquid-crystal (LC) compositions with a chiral nematic or cholesteric structure are used in surface-stabilized cholesteric texture (SSCT) and polymer-stabilized cholesteric texture (PSCT) displays. A cholesteric LC medium for these devices can be prepared by doping a nematic LC mixture with a chiral dopant having enough high twisting power [1, 2]. The pitch $\boldsymbol{P}$ of the induced cholesteric helix is then given by the concentration $\boldsymbol{C}$ and the helical twisting power $\boldsymbol{\beta}$ of the chiral dopant in accordance with Eq. (1)

$$\boldsymbol{P} = (\boldsymbol{\beta} \cdot \boldsymbol{C})^{-1} \quad (1)$$

The reflection wavelength $\boldsymbol{\lambda}$ is given by the pitch $\boldsymbol{P}$ of the cholesteric helix and the mean refractive index $\boldsymbol{n}$ of the cholesteric LC in accordance with following Eq. (2):

$$\boldsymbol{\lambda} = \boldsymbol{n} \cdot \boldsymbol{P} \quad (2)$$

For use in SSCT and PSCT displays, the chiral dopants should have the highest possible helical twisting power and low temperature dependence of the reflection wavelength, high chemical, thermal and electric stability and good solubility in the LC host phase and do not impair the liquid-crystalline properties of the LC medium. Besides, they should have minimum negative effect on the electro-optical properties of the host phase. However, in practice it is very difficult to achieve favourable values for all the above-mentioned parameters using only one chiral dopant. That is why in cholesteric LC composition for SSCT or PSCT

Electronic supplementary material The online version of this article (doi:10.1007/s11224-015-0700-y) contains supplementary material, which is available to authorized users.

✉ Svitlana V. Shishkina
sveta@xray.isc.kharkov.com

Victoria V. Lipson
lipson@ukr.net

[1] State Scientific Institution "Institute for Single Crystals" of the National Academy of Sciences of Ukraine, Kharkiv 61001, Ukraine

[2] Medicinal Chemistry Department, State Institution "V.Ya. Danilevsky Institute for Endocrine Pathology Problems" of the National Academy of Medical Sciences of Ukraine, Artema St., 10, Kharkiv 61002, Ukraine

[3] V. N. Karazin Kharkiv National University, 4 Svobody sq., Kharkiv 61122, Ukraine

displays, multi-component mixtures of different optically active compounds have found application [3, 4].

Preferred chiral dopants are compounds from a series of sugar derivatives [5, 6], binaphthols (BINOLs) [7, 8], tetraaryl-1,3-dioxolane-4,5-dimethanols (TADDOLs) [4, 9, 10], lactic acids [11], cholesterol ethers [12], terpenes [13, 14], amino acids [15] and spiro-biindanes [16, 17]. Dianhydrosorbitols, TADDOLs and BINOLs exhibit the best characteristics [3, 4, 9]. Their helical twisting power values are more than 65–70 μm^{-1}. But one of the critical characteristics of such compositions is the temperature gradient of the induced helical pitch. To maintain a certain colour when the temperature changes in such compositions are added compensating components. This significantly affects the physical properties of the LC materials [3, 6–10].

Recently 16-ylidene derivatives of the steroids from androstenone and estrone series have been invented as new chiral dopants with helical twisting power $\boldsymbol{\beta} \sim 32$–$56$ μm^{-1}, with high light stability and low temperature dependence of the reflection wavelength [18, 19]. Cholesteric LC compositions in which the chiral component comprised only one from above-mentioned chiral compounds in an amount 7.2–12.8 % demonstrated selective reflection of light in the visible range from blue to red. However, the proportion of optically active component in commercial cholesteric LC media is <10 %, in particular preferably <7 % [3, 4, 6].

All dopants with high helical twisting power discussed above (TADDOLs, BINOL's, sugar derivatives and steroids) despite the differences in their structure have a number of common features such as chiral scaffold and extended easily polarizable π-electron fragment (promesogenic fragment). Within each series of these dopants, $\boldsymbol{\beta}$ value depends significantly on the length of promesogenic fragment, the mutual arrangement of this fragment and a chiral core, and the spatial structure of the molecule as a whole.

For these reasons, we have synthesized new group of chiral dopants (**4**-**8**) (for structures see Fig. 1) based on allobetuline (**2**) which was derived from betulin (3β,28-dihydroxy-20(29)-lupen) (**1**). The later is pentacyclic triterpenoid from lupane series easily available from renewal natural resources such as black- and white-barked birch trees (e.g. *Betula verrucosa, Betula pubescens, Betula alba*) with yields 10–40 % (dry weight). Transformation of the isopropenyl and hydroxymethyl fragments of betulin (**1**) into tetrahydrofuran moiety of allobetuline (**2**), as a result of the Wagner–Meerwein rearrangement, makes the ring **A** in this scaffold the most reactive [20, 21]. The aim of this study is elucidation relationship between spatial structure of the new chiral dopants based on allobetuline derivatives (**4**–**8**) with different substituents in the ring **A** and their helical twisting power $\boldsymbol{\beta}$ in the nematic matrix.

Experimental

Materials and methods

All commercially available reagents and solvents were purchased from Sigma-Aldrich and used without further purification. ^{1}H NMR and ^{13}C NMR spectra were recorded on a Varian Mercury-200 spectrometer 200 MHz and Varian Mercury-400 spectrometer 100 MHz, respectively, with TMS as an internal reference and $CDCl_3$ as a solvent. The IR spectra were performed between 4000 and 400 cm^{-1} on a Perkin Elmer Spectrum One FT-IR spectrometer using the KBr pellets. Elemental analyses were carried out on an EA 3000 Eurovector elemental analyser. Melting points were determined on a Kofler hot bench. The progress of reactions and also the purity of the obtained compounds were monitored by TCL on Alugram® Xtra SIL G/UV_{254} plates with hexane—ethylacetate (10:1) as an eluent.

Synthesis

Allobetulin (**2**) and allobetulon (**3**) were synthesized from commercially available betulin (**1**) according to the well-known procedures published previously [22].

(E)-2-(4-chlorobenzylidene)allobetulone (**4**) A mixture of 1 g (2.3 mmol) of allobetulon (**3**) and 0.35 g (2.5 mmol) 4-chlorobenzaldehyde in 30 mL 2-methoxyethanol, containing a catalytic amount of potassium hydroxide (Scheme 1), was refluxed for 8 h. The solvent was evaporated under reduced pressure to a volume of 10 mL, the residue was cooled, and the white amorphous precipitate was filtered off. Yield 1 g (78 %), mp 173–174 °C; IR (KBr, cm^{-1}) 2994-2861 (CH_2,CH_3), 1683 (CO), 1602 (C=C), 1036 (COC). ^{1}H NMR (400 MHz, $CDCl_3$) δ 7.40 (s, 1H, CH_{vinil}), 7.33 (s, 4H, Ar–H), 3.75 (s,1H, 28-CH_B), 3.52 (s, 1H, 19-CH), 3.42 (s, 1H, 28-CH_A), 3.01 (d, $J = 16.1$ Hz, 1H, 1-CH*e*), 2.19 (d, $J = 15.1$ Hz, 1H, 1-CH*a*), 1.13, 1.10, 0.99, 0.94, 0.91, 0.78 (all s, 21H, $7 \times CH_3$). ^{13}C NMR (101 MHz, $CDCl_3$) δ 208.19, 136.19, 135.09, 134.71, 134.61, 131.73, 128.96, 88.18, 71.56, 53.29, 49.31, 47.08, 45.52, 44.93, 41.77, 41.10, 40.75, 37.03, 36.86, 36.58, 34.59, 32.99, 29.75, 29.11, 26.84, 26.70, 26.54, 24.85, 22.64, 22.09, 20.61, 16.41, 15.54, 13.73. Anal. ($C_{37}H_{51}ClO_2$): Calcd. C, 78.90; H, 9.13; Cl, 6.29; found C, 78.85; H, 9.10; Cl, 6.63. Single crystals suitable for the X-ray diffraction were prepared by crystallization of the compound (**4**) from ethanol.

(E)-2-(4-chlorophenylmethylidene) allobetuline (**5**) To suspension of 0.5 g (0.9 mmol) of α,β-unsaturated ketone (**4**) in 10 mL of propan-2-ol, 0.1 g (2.7 mmol) of $NaBH_4$

Fig. 1 Structure of investigated compounds

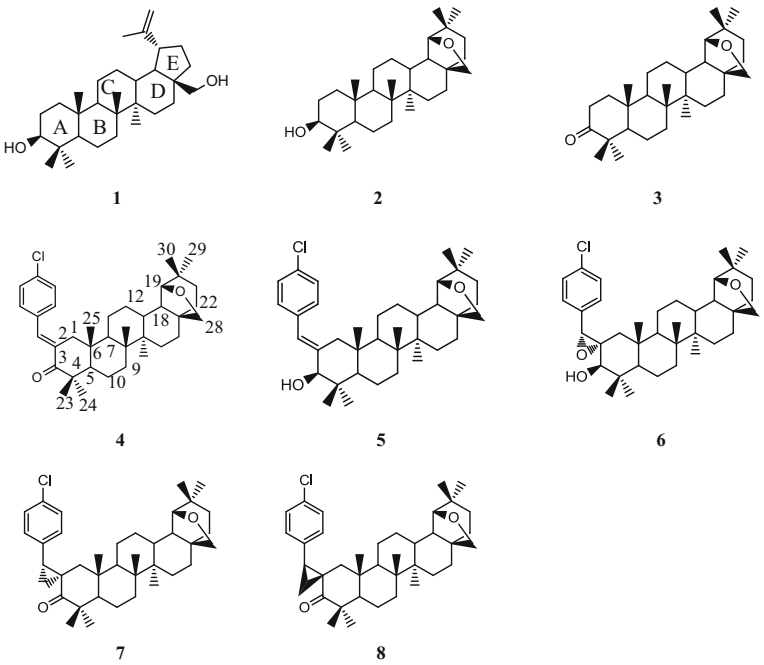

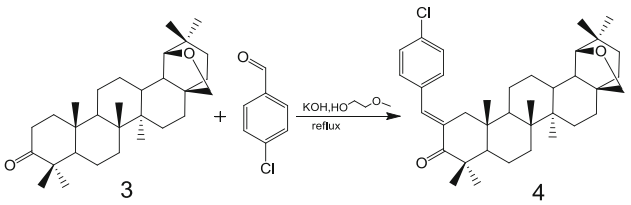

Scheme 1 Synthesis of (*E*)-2-(4-chlorobenzylidene)allobetulone (**4**)

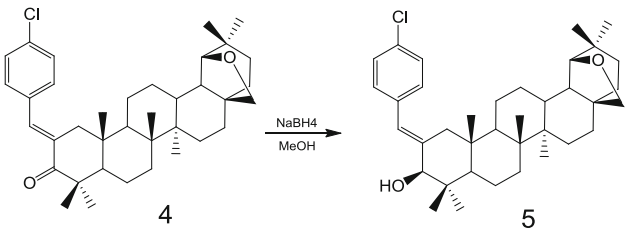

Scheme 2 Synthesis of (*E*)-2-(4-chlorobenzylidene)allobetuline (**5**)

was added under stirring (Scheme 2). The reaction mixture was stirred under room temperature (RT) for 16 h and then was diluted by water (20 mL) and stirred for 1 h. The white amorphous precipitate was filtered off. Yield 0.5 g (99 %), mp 233–235 °C; IR (KBr, cm^{-1}) 3368 (OH), 2967-2658 (CH_2–CH_3), 1650 (C=C), 1036 (COC). ^{1}H NMR (400 MHz, $CDCl_3$) δ 7.25 (d, $J = 8.3$ Hz, 2H, Ar–H), 7.11 (d, $J = 8.2$ Hz, 2H, Ar–H), 6.64 (s, 1H, CH_{vinil}), 3.83 (s, 1H, 3-CH*a*), 3.73 (d, $J = 7.8$ Hz, 1H, 28-CH_B), 3.48 (s, 1H, 19-CH), 3.41 (d, $J = 7.7$ Hz, 1H, 28-CH_A), 2.93 (d, $J = 12.7$ Hz, 1H, 1-CH*e*), 1.10, 0.90, 0.76, 0.71, 0.66 (all s, 21H, 7 × CH_3). ^{13}C NMR (101 MHz, $CDCl_3$) δ 141.48,

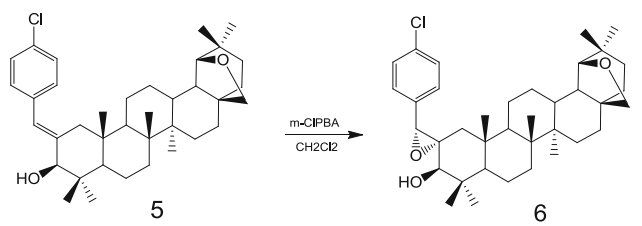

Scheme 3 Synthesis of (2*R*,3*R*)-3-(4′-chlorophenyl)-2,2′-spiro-oxyranoallobetuline (**6**)

136.77, 131.92, 130.35, 128.51, 121.84, 88.15, 81.22, 71.44, 64.60, 56.27, 50.59, 47.02, 42.32, 41.82, 41.65, 41.04, 40.98, 40.64, 36.95, 36.46, 34.34, 33.97, 32.90, 29.02, 28.73, 26.65, 26.54, 26.45, 25.56, 24.75, 21.38, 18.58, 16.74, 15.79, 13.69. Anal. ($C_{37}H_{53}ClO_2$): Calcd. C, 78.62; H, 9.45; Cl, 6.27; found C, 78.58; H, 9.39; Cl, 6.22.

(2R,3R)-3-(4′-chlorophenyl)-2,2′-spiro-oxyranoallobetuline (**6**) To solution of 0.3 g (0.53 mmol) of allobetuline derivative (**5**) in dichloromethane (5 mL), 0.1 g (0.59 mmol) of *m*-chloroperoxybenzoic acid (*m*-ClPBA) was added (Scheme 3), and reaction mixture was stirred for 14 h under RT. At the end of reaction, mixture was washed with the 10 % solution of $NaHCO_3$ in water (3 × 10 mL). The organic phase was dried over anhydrous magnesium sulphate, and the solvent was removed in vacuo. Yield 0.3 g (97 %), mp 244–246 °C; IR (KBr, cm^{-1}) 3559 (OH), 2993-2855 (CH_2, CH_3), 1039 (COC). ^{1}H NMR (400 MHz, $CDCl_3$) δ 7.25 (d, $J = 8.0$ Hz, 2H, Ar–H), 7.14 (d, $J = 8.2$ Hz, 2H, Ar–H), 4.35 (s, 1H, 3′-CH), 3.64 (d, $J = 7.3$ Hz, 1H, 28-CH_B), 3.53 (s, 1H, 3-CH*a*), 3.39 (s, 1H,

19-CH), 3.34 (d, $J = 7.0$ Hz, 1H, 28-CH_A), 2.05(s, 1H, OH), 1.04, 0.82, 0.76, 0.70, 0.29 (all s, 21H, 7 × CH_3). ^{13}C NMR (101 MHz, $CDCl_3$) δ 134.74, 133.36, 128.35, 128.15, 128.03, 87.84, 78.46, 71.14, 66.21, 59.97, 55.69, 50.57, 46.71, 41.35, 40.70, 40.63, 39.77, 39.49, 36.66, 36.17, 33.89, 33.59, 32.60, 28.74, 28.63, 26.24, 26.13, 24.48, 20.85, 17.73, 16.58, 16.47, 15.51, 13.37. Anal. ($C_{37}H_{53}ClO_3$): Calcd. C, 76.45; H, 9.19; Cl, 6.10; found C, 76.38; H, 9.13; Cl, 6.04.

(1S,2S)- and (1R,2R)-1-(4′-chlorophenyl)-2,2′-spiro-cyclopropylallobetulone (**7, 8**) A mixture of 0.08 g (1.8 mmol) 50 % sodium hydride and 0.43 g (1.95 mmol) of trimethylsulphoxonium iodide in dry DMF (15 mL) was stirred until hydrogen evolution (Scheme 4). Then to mixture heated until 60 °C, 0.5 g (0.9 mmol) of α,β-unsaturated ketone (**4**) was added. After 0.5 h, this reaction mixture was diluted by water (50 mL) and white amorphous precipitate was filtered off. The precipitate was dried at 50 °C, and a mixture of isomers was divided by column chromatography with silica gel and dichloromethane as eluent. Yield (**7**) 0.35 g (69 %), mp 252–253 °C; IR (KBr, cm^{-1}) 2987-2861 (CH_2, CH_3), 1670 (C=O), 1038 (COC). (**7**) ^{1}H NMR (400 MHz, $CDCl_3$) δ 7.23 (d, $J = 6.0$ Hz, 2H, Ar–H), 6.97 (d, $J = 8.1$ Hz, 2H, Ar–H), 3.70 (d, $J = 7.4$ Hz, 1H, 28-CH_B), 3.45 (s, 1H, 19- CH), 3.39 (d, $J = 7.6$ Hz, 1H, 28-CH_A), 2.90 (t, $J = 8.2$ Hz, 1H, 2′-CH), 1.10, 1.05, 0.89, 0.87,0.85, 0.74, 0.53 (all s, 21H, 7 × CH3). ^{13}C NMR (101 MHz, $CDCl_3$) δ 217.36, 135.26, 132.44, 130.43, 128.07, 87.79, 71.17, 54.24, 48.30, 46.68, 45.92, 41.36, 40.66, 40.49, 40.28, 37.05, 36.78, 36.67, 36.18, 34.16, 32.82, 32.63, 32.14, 29.62, 28.75, 26.35, 26.27, 26.18, 24.46, 22.98, 22.85, 21.22, 19.97, 15.39, 14.60, 13.25. Anal. ($C_{38}H_{53}ClO_2$): Calcd C, 79.06; H, 9.25; Cl, 6.14; found C, 79.01; H, 9.21; Cl, 6.11. Yield (**8**) 0.15 g (29 %) mp 115–116 °C; IR (KBr, cm^{-1}) 2996- 2869 (CH_2, CH_3), 1683 (C=O), 1038 (COC). ^{1}H NMR (400 MHz, $CDCl_3$) δ 7.25 (d, $J = 7.8$ Hz, 1H, Ar–H), 7.03 (d, $J = 7.8$ Hz, 1H, Ar–H), 3.73 (d, $J = 7.3$ Hz, 1H, 28-CH_B), 3.47 (s, 1H, 19-CH), 3.41 (d, $J = 7.8$ Hz, 1H, 28-CH_A), 2.71 (d, $J = 7.7$ Hz, 1H, 2́-CH), 1.10, 1.06, 0.98, 0.94, 0.89, 0.83, 0.73 (all s, 21H, 7 × CH_3). ^{13}C NMR (101 MHz, $CDCl_3$) δ 216.96, 135.80, 132.31, 130.75, 129.57, 128.40, 127.68, 87.80, 71.21, 54.29, 48.30, 46.68, 46.05, 44.58, 41.38, 40.73, 40.31, 37.54, 36.66, 36.21, 34.14, 33.73, 32.78, 32.63, 31.31, 29.42, 28.74, 27.46, 26.29, 26.18, 24.46, 22.80, 21.38, 20.19, 15.43, 15.40, 13.33. Anal. ($C_{38}H_{53}ClO_2$): Calcd. C, 79.06; H, 9.25; Cl, 6.14; found C, 78.99; H, 9.23; Cl, 6.13.

Determination of a helical twisting power (***β***) for compounds (**4-8**) in 4-pentyl-4′-cyanobiphenyl nematic solvent

Twisting power was calculated according to the formula (3)

$$\beta = (P_{\mathrm{Tred}} \cdot C \cdot r)^{-1}, \quad (3)$$

where ***C***—chiral dopant concentration, $\boldsymbol{P}_{\mathbf{Tred}}$—the pitch of a chiral dopant at reduced temperature T_{red} ($T_{\mathrm{red}} = (T_{\mathrm{iso}} + 273)$ 0.98–273, T_{iso} is the temperature of the phase transition cholesteric—isotropic liquid, *r*—enantiomeric purity of chiral dopant (for all compounds (**4-8**) $r = 1$). Value of $\boldsymbol{P}_{\mathrm{Tred}}$ was determined by the method published early [23, 24]. The twisting power data are given in Table 1.

X-ray diffraction study

X-ray diffraction studies were performed on an automatic «Xcalibur 3» diffractometer (graphite monochromated MoK_α radiation, CCD-detector, ω-scanning). The structures were solved by direct method using SHELXTL package [25]. Positions of the hydrogen atoms were located from electron density difference maps and refined by "riding" model with U_{iso}=nU_{eq} of the carrier atom ($n = 1.5$ for methyl and hydroxyl groups and $n = 1.2$ for other hydrogen atoms) for (**4**), (**5**) and (**7**) structures. Hydrogen atoms were refined using isotropic approximation in the (**6**) structure. The crystallographic data and experimental parameters are listed in Table 2. Final atomic coordinates, geometrical parameters and crystallographic data have been deposited with the Cambridge Crystallographic Data Centre, 11 Union

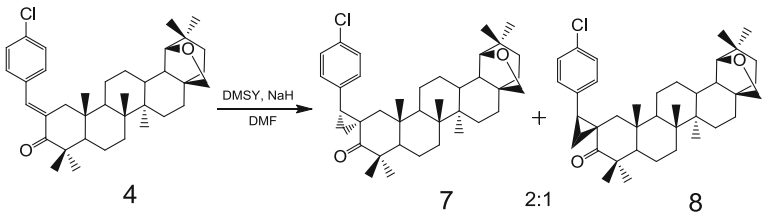

Scheme 4 Synthesis of (1*S*,2*S*)- and (1*R*,2*R*)-1-(4′-chlorophenyl)-2,2′-spiro-cyclopropylallobetulone (**7, 8**)

Table 1 Twisting power (***β***) for compounds (**4-8**)

Compound	(**4**)	(**5**)	(**6**)	(**7**)	(**8**)
$\lvert\boldsymbol{\beta}\rvert$ (mkm^{-1} mol $pats^{-1}$)	29.66 ± 1.4	71.38 ± 3.4	84.25 ± 3.7	57.75 ± 2.6	3.38 ± 0.16

Table 2 Crystallographic data and experimental parameters for compounds (**4-7**)

Parameter	(**4**)	(**5**)	(**6**)	(**7**)
Unit cell dimensions				
a (Å)	14.851 (2)	23.895 (3)	6.5079 (5)	6.521 (1)
b (Å)	6.4337 (9)	9.863 (1)	21.598 (1)	21.438 (5)
c (Å)	17.181 (2)	19.071 (2)	23.101 (2)	23.274 (3)
α (°)	90.0	90.9	90.0	90.0
β (°)	108.50 (2)	124.73 (1)	90.0	90.0
γ (°)	90.0	90.0	90.0	90.0
V (Å^3)	1556.8 (4)	3694.3 (7)	3247.0 (4)	3254 (1)
F (000)	612	1484	1264	1256
Crystal system	Monoclinic	Monoclinic	Orthorhombic	Orthorhombic
Space group	$P2_1$	C2	$P2_12_12_1$	$P2_12_12_1$
Z	2	2	4	4
T (K)	293	100	293	293
μ (mm^{-1})	0.154	0.352	0.152	0.149
D_{calc} (g/cm^3)	1.202	1.245	1.189	1.178
$2\Theta_{max}$ (°)	60	50	60	50
Measured reflections	15,553	11,883	18,363	13,223
Independent reflections	8715	5963	9090	5715
R_{int}	0.063	0.061	0.027	0.066
Reflections with $F > 4\sigma(F)$	3044	4184	6332	3376
Parameters	368	410	582	377
R_1	0.072	0.100	0.048	0.063
wR_2	0.176	0.270	0.110	0.146
S	0.843	1.002	0.979	0.940
CCDC number	1,053,941	1,053,942	1,053,943	1,053,944

Road, Cambridge, CB2 1EZ, UK (Fax: +44 1223 336033; e-mail: deposit@ccdc.cam.ac.uk). The deposition numbers are given in Table 2.

Results and discussion

From the data in the Table 1 is followed that the twisting power $|\beta|$ varies significantly from a cinnamoyl derivative (**4**) to spiro-compounds (**6**) and (**8**). Apparently, the greatest influence on this index has not conjugated chain length (in the case of compound (**4**), conjugated π-electron fragment is the largest and the value of $|\beta|$ is small), and cycle **A** conformation in the triterpenoid scaffold. In order to reveal basic structural attribute that affects the twisting power, we examined the features of the spatial structure of the compounds (**4**-**8**) by NMR ^{1}H and X-ray diffraction methods.

NMR spectral data

In NMR ^{1}H spectra of all compounds (**4**–**8**), a multiplet from aromatic protons is observed at δ 7.02–7.35 ppm. Protons in the tetrahydrofuran ring gave rise to AB doublets in the region δ 3.47–3.79 ppm from the methylene group and a singlet at δ 3.35–3.53 ppm from the CH group. Multiplets from the CH and CH_2 protons of the lupane core are located at δ 1.08–1.74 ppm, and protons of the seven methyl groups resonated as singlets in the region δ 0.74–1.25 ppm. Signals from the vinylic protons of the 2-ylidene derivatives (**4**) and (**5**) are observed as a singlet at δ 7.40 and 6.64 ppm, respectively. In the transition from α,β-unsaturated ketone (**4**) to allyl alcohol (**5**), upfield shift of the equatorial proton doublet for C(1)H_2 group is observed. In the spectrum of the compound (**4**), it resonates at 3.01, but in the spectrum of the hydroxy derivative (**5**), this doublet is found at 2.93 ppm. A doublet of the axial proton also demonstrates upfield shift and gets on the screen signals of CH, CH_2, CH_3 groups.

In the case of compound (**5**) appears upfield singlet of methyl group with chemical shift 0.66 ppm, but signal at 0.98 ppm, which is presented in α,β-unsaturated ketone (**4**) spectrum, is not found. Apparently, this singlet can be attributed to resonance of the Me(25) group (C24 in X-ray numbering, see below) because it is shielded by vinyl moiety due to changes in the conformation of ring **A**. Our assumption regarding the spatial convergence of these

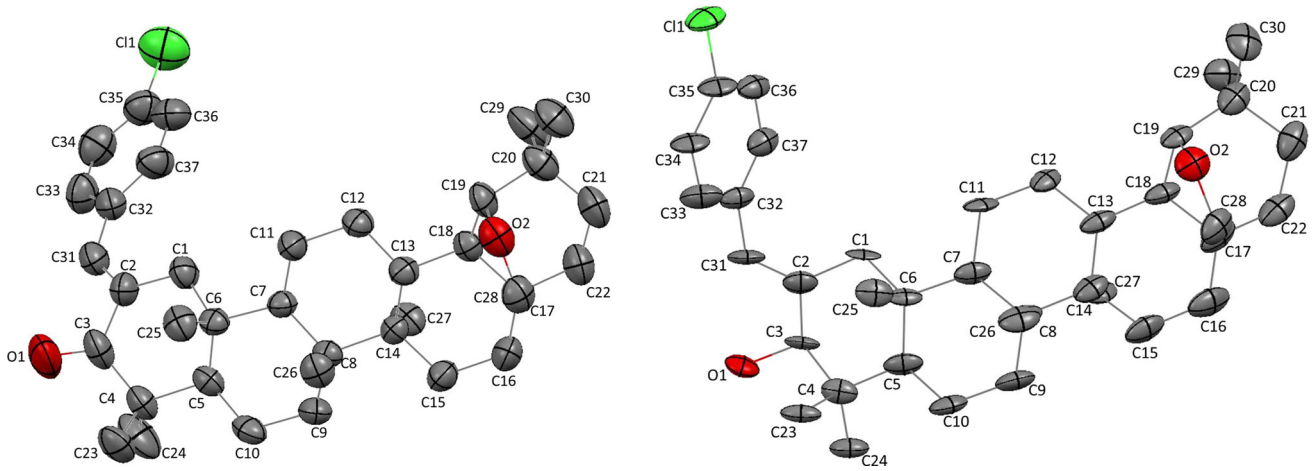

Fig. 2 Molecular structure of the compounds (**4**) (on the *left*) and (**5**) (on the *right*). Hydrogen atoms are omitted for clarity. Thermal ellipsoids are shown at 50 % probability level

fragments is confirmed by X-ray analysis of the compound (**5**) single crystal (see Fig. 2). Thus, the stereochemistry of the substituent on the C(2) atom and the ring **A** conformation significantly affect the chemical shift of the Me(25) group. This tendency to upfield shift of the Me(25) group signal is clearly seen in the series of compounds (**5**-**7**). The reason of this phenomenon is in the shielding by π-electron system of the substituent at C2 atom in cycle **A** protons of Me(25) group. As mentioned above, in the compound (**5**) the vinyl fragment and the Me(25) group are arranged spatially close to one another. However, in the case of compounds (**6**) and (**7**), protons of the Me(25) group are shielded by π-electron system of the 4′-chlorophenyl radical (see Fig. 3). Chemical shifts of these CH_3 groups in the spectra of compounds (**6**) and (**7**) are 0.29 and 0.56 ppm, respectively. Apparently, such a difference in chemical shifts associated with different conformation of ring **A** in compounds (**6**) and (**7**). In the *β*-spiro-cyclopropane's spectrum (**8**), chemical shift of the Me(25) group appeared at 0.98 ppm. Perhaps, in this case the aryl radical and the methyl group are removed from each other.

Thus, comparing the value of twisting power of the compounds (**4**-**8**) to their spatial structure can be noted that the closer to each other are arranged the π-electron system of the substituent at C(2) atom in the ring **A** and methyl group Me(25), the greater is value |***β***|.

Molecular structure in solid

The steric structure of unsaturated ketone (**4**) was unambiguously determined by X-ray study of its single crystal (Fig. 2). The C1–C2–C3–C4–C21–C22 six-membered ring adopts a *twist–boat* conformation. The puckering parameters [26] and deviations of the corresponding atoms from the mean plane of the remaining atoms of the ring are given in Table 3. The O=C–C=C–Ph fragment is supposed to be conjugated what has to result in its planarity. However, the planar structure of this fragment causes the appearance of essential repulsion between the ring **A** and aromatic ring of the substituent at the C2 atom what is confirmed by a lot of shortened intramolecular contacts between them (Table 4). To compensate such repulsion, there is the disturbance of conjugation between two exocyclic double bonds and between aromatic ring and C=C bond (the O1–C1–C2–C31 and C2–C31–C32–C37 corresponding torsion angles are given in Table 3), the twisting of the C=C double bond (the C1–C2–C3–C32 torsion angle) and the increasing of the C3–C2–C31 and C2–C31–C32 bond angles (Table 4) as compared to standard value 120° in this fragment. At that case, the methyl group C24 interacts with the exocyclic C=O bond, what can be considered as the C–H···π weak intramolecular hydrogen bond (H···C 2.53 Å C–H···C 120°). It is known that the formation of the interaction between two atoms is accompanied by the existence of the (3−1) bond critical point (BCP) of the electron density distribution within the Bader's theory "Atoms in Molecules" [27]. Application of the Espinosa's formula [28] to the analysis of the (3,−1) BCP characteristics allows estimate the interaction energy. Thus, the energy of the C24–H···C1 interaction is 2.21 kcal/mol and corresponds to a weak C–H···π hydrogen bond.

The reduction of the carbonyl group to the hydroxyl one results in the shortening of the conjugated system in the compound (**5**) (Fig. 2). This dramatically changes the conformation of the ring **A**, which adopts a *chair* conformation (Table 3). In addition, the conjugation between exocyclic double bond and aromatic ring becomes weaker, leading to the more turn of the π-systems relatively each other (the C2–C31–C32–C37 torsion angle, Table 3). The decreasing of the repulsion between aromatic ring and ring

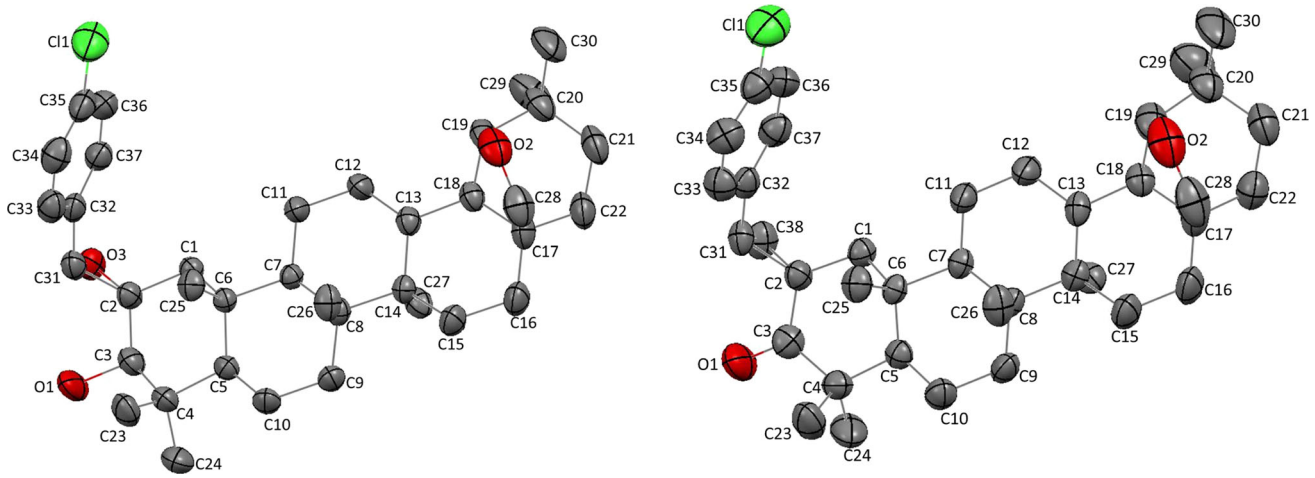

Fig. 3 Molecular structure of the compounds (**6**) (on the *left*) and (**7**) (on the *right*). Hydrogen atoms are omitted for clarity. Thermal ellipsoids are shown at 50 % probability level

Table 3 Some geometric parameters for the (**4–7**) molecules

	(4)	(5)	(6)	(7)
Puckering parameters				
S	0.80	1.14	1.10	0.81
Θ	70.0	4.3	3.1	33.4
Ψ	18.8	5.9	3.0	4.5
Deviations of atoms				
C21	−1.08			
C22	−0.80			
C1		0.69	0.60	
C4		−0.66	−0.69	0.70
Bond angles (°)				
C3–C2–C31	126.3 (4)	124.1 (7)	122.4 (2)	120.8 (3)
C2–C31–C32	131.0 (4)	128.4 (7)	123.0 (2)	121.3 (3)
Torsion angles (°)				
O1–C1–C2–C31	−40.0 (6)	8 (1)	18.7 (2)	37.3 (5)
C1–C2–C31–C32	−167.8 (4)	179.4 (7)	157.9 (2)	141.1 (3)
C2–C31–C32–C37	−19.3 (7)	50 (1)	59.7 (3)	65.7 (5)

Table 4 Some intramolecular contacts in the (**4**)-(**7**) molecules

	(**4**)	(**5**)	(**6**)	(**7**)
H24···C1	**2.53**	3.36	3.35	**2.80**
H24···C2	**2.78**	**2.62**	**2.63**	**2.57**
H24···C31	4.00	2.92	**2.75**	2.93
H24···C32	5.13	3.32	**2.81**	3.12
H24···C33	6.39	3.62	**2.82**	3.14
C24···C1	**3.11**	3.77	3.69	3.34
H3a···H37	**2.31**	**2.27**	2.42	2.49
H3b···H37	**2.23**	3.14	3.44	3.53
H37···C3	**2.59**	2.93	3.10	3.22
C37···C3	**3.16**	**3.28**	**3.29**	**3.35**
H3a···C32	3.28	**2.67**	**2.70**	**2.62**
H3a···C37	**2.81**	**2.56**	**2.58**	**2.57**

Shortened contacts are marked by bold type. The van der Waals radius sum is 2.87 Å for C···H contact and 2.34 Å for H···H contact

A is confirmed by the reduction of quantity of the shortened contacts and their weakening (Table 4) and the absence of the double bond twistedness (the C1–C2–C31–C32 torsion angle). The methyl group C24 forms the C–H···π intramolecular interaction with the sp^2-hybridizated C2 atom. It can be noticed that such change in the intramolecular interactions is accompanied by sharply increasing of the twisting power (***β***) (Table 1).

The formation of the three-membered rings in the compounds (**6**) and (**7**) (Fig. 3) does not change the hybridization of the C2 atom. It is well known that the small rings such as cyclopropane and epoxide are formally saturated systems, but their behaviour is very close to the behaviour of unsaturated bonds. The carbon atoms of cyclopropane and epoxide rings were supposed to have sp^2-hybridization in spite of the formation of four bonds [29]. The unhybridizated π-orbitals of the three-membered ring lie in the ring's plane and do not take part in the conjugative interactions with aromatic substituent. Additionally the sp^2-hybridization of the C2 atom requires its planar environment. Taking into account that this atom centred on four bonds, this requirement results in the orthogonal orientation of the C1, C2, C3 and O3, C31, C2 planes (dihedral angle between planes is 87°). The *p*-chlorophenyl substituent deviates from the plane of the C1, C2, C31 atoms and is turned relatively to the C2–C31 bond of the epoxide ring (Table 3) due to enough free rotation around the C31–C32 bond in the compound (**6**). The C2–C31 bond length (1.484(3) Å) is shorter than the mean value of the C–C bond [30] 1.510 Å in the cyclopropane, and the lengths of the O3–C31 and

O3–C2 bonds are very close to each other (1.445(2) Å and 1.451(2) Å, respectively). The ring **A** adopts a *chair* conformation (Table 3) in the compound (**6**) similar to one in (**5**). In summary, such structure of this fragment creates conditions for the approach of the chiral scaffold and the π-electron substituent, leading to the formation a lot of the intramolecular interactions between C24 methyl group as proton donor and epoxyed and aromatic rings as proton acceptor (Table 4). It can be assumed that these interactions are enough weak each taken separately, but their total energy is appreciable. This allows stabilizing reciprocal orientation of scaffold and substituent, leading to the increasing of the twisting power (Table 1).

The oxidation of the hydroxyl group to carbonyl causes the change of the conformation of the ring **A** in the compound (**7**). The presence of two sp^2-hybridizated atoms in the neighbouring positions and absence of steric repulsion owing to orthogonal orientation of the C1, C2, C3 and C38, C31, C2 planes lead to the ring **A** adopts a *sofa* conformation. Such conformation of this ring promotes the approaching of the C24 methyl and the carbonyl groups. At that, the replacement of the oxygen atom by the carbon atom in the three-membered ring results in the essential inequality of the cyclopropane bond lengths. The C2–C31 bond (1.547(5) Å) is significantly longer as compared to the mean value (1.510 Å), and the C38–C31 bond is shorter (1.471(4) Å). As a result, the C24 methyl group again forms the C–H···π interaction with nearer π-systems of the carbonyl group and the C2 atom (Table 4). The twisting power decreases in compound (**7**).

Unfortunately, a single crystal of compound (**8**) was not obtained. For this reason, the choice of its most stable conformation was carried out using quantum-chemical calculations (Fig. 4).

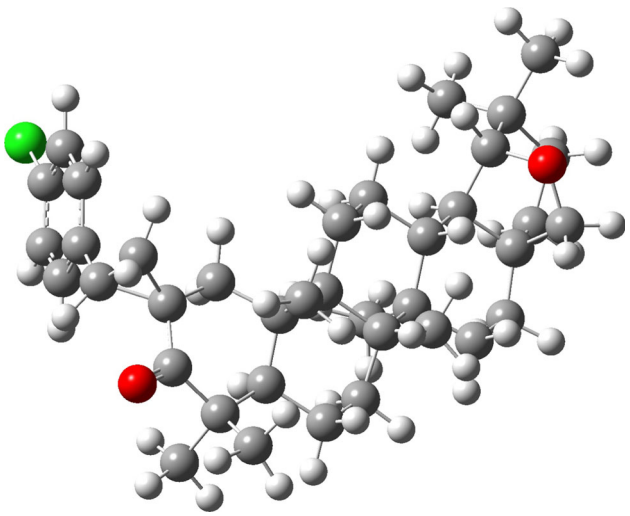

Fig. 4 Molecular structure of compound (**8**) optimized by m05-2x/cc-pvdz method

As a result, it was found that the conformation of the ring A is saved for the minor diastereomer (a *sofa* conformation). However, the distance between the Me(25) group (hydrogen atom at C24 according X-ray numbering) and aryl fragment increases noticeably due to orientation of p-chlorophenyl substituent (the H24···C31 distance is 3.89 Å, H24···C32 4.95 Å and H24···C33 5.48 Å). It can be noted also the shortening of the H24···C2 distance (2.49 Å) as compared to one in molecules **4-7**. This probably leads to a sharp decrease in the value $|\beta|$.

Conclusion

Starting from 2-(4′-chlorophenyl)methylidene derivative of allobetulon, new series of chiral dopants for cholesteric liquid-crystal compositions were synthesized. Their spatial structure study by NMR ^{1}H, X-ray diffraction methods and quantum-chemical calculations and comparison of these results with the value of twisting power $|\beta|$ suggest that the closer to each other are arranged the π-electron system of the substituent at C(2) atom in the ring **A** and Me(25) group, the greater is value $|\beta|$. Spatial convergence of these fragments favours the existence of ring **A** in the *chair* conformation.

Acknowledgments This work was performed using computational facilities of joint computational cluster of SSI "Institute for Single Crystals" and Institute for Scintillation Materials of National Academy of Science of Ukraine incorporated into Ukrainian National Grid.

References

1. Yang DK, Huang XY, Zhu YM (1997) Bistable cholesteric reflective displays: materials and drive schemes. Annu Rev Mater Sci 27:117–146
2. Ren H, Wu ST (2002) Reflective reversed-mode polymer stabilized cholesteric texture light switches. J Appl Phys 92:797–800
3. Kojima A, Shimano F (2013) Liquid-crystalline medium and liquid-crystal display having high twist. US Patent 83,494,15B,2
4. Seed A, Walsh M, Doane JW, Khan A (2004) New high twisting power material for use as a single asymmetric dopant in cholesteric displays with a temperature independence of the helical twisting power. Mol Cryst Liq Cryst 410:201–208
5. Parri OL, Nolan P, Farrand LD, May A (2001) Chiral dopants. US Patent 621,779,2
6. Bauer M, Boeffel C, Kuschel F, Zaschke H (2006) Evaluation of chiral dopants for LCD applications. J Soc Inform Display 14:805–812
7. Farrand LD (2010) Chiral compounds. Patent US 777,180,0
8. Farrand LD, Saxton PE (2011) Chiral binaphthyl sulfates for use as liquid crystal materials. US Patent 794,306,1
9. Kirsch P, Tangerbeck A, Pauluth D (2006) Chiral compounds III. US Patent 704,134,5
10. Doane JW, Khan AA, Seed AJ (2004) Chiral additives for cholesteric displays. US Patent 683,078,9
11. Bobrovsky A, Ryabchun A, Cigl M, Hamplová V, Kašpar M, Hampl F, Shibaev V (2014) New azobenzene-based chiral-

photochromic substances with thermally stable Z-isomers and their use for the induction of a cholesteric mesophase with a phototunable helix pitch. J Mater Chem C 2:8622–8629
12. Vill V, Fischer F, Thiem J (1988) Helical twisting power of carbohydrate derivatives. Z Naturforsch 43a:1119–1125
13. Drushlyak TG, Kutulya LA, Pivnenko NS, Shkolnikova NI, Vashchenko VV (2001) Diastereomeric 2-(4-carboxy-benzylidene)-*p*-menthane-3-one derivatives as components of LC systems with induced helical structure. Mol Cryst Liq Cryst A 364:691–701
14. Kutulya LA, Vashchenko VV, Semenkova GP, Shkolnikova NI, Drushlyak TG, Goodby JW (2001) Chiral organic compounds in liquid crystal systems with induced helical structure. Mol Cryst Liq Cryst 361:125–134
15. Radley K, Lilly GJ (1993) Potassium salts of acylated amino acids as chiral dopants and hosts in the formation of amphiphilic cholesteric liquid crystals. Molecular crystals and liquid crystals science and technology, sec. Mol Cryst Liq Cryst 231:183–190
16. Cheng CH, Wang KC, Wu CM, Cheng KL, Liu SH, Chin CL (2013) Chiral dopants, liquid crystal matrix and manufacturing method thereof and liquid crystal display. US Patent 8449953
17. Welter TR (2008) Temperature compensating chiral dopants. US Patent 73,293,68B,2
18. Yaremenko FG, Pivnenko NS, Kutulya LA, Kondratyuk ZhA, Novikova NB, Shkolnikova NI (2009) New steroid α, β-unsaturated ketones as chiral components of induced cholesteric liquid crystal systems. Rus Chem Bull 58:1072–1083
19. Yaremenko FH, Taidakov IV, Sheshenko ZhO, Vakula VM, Shkolnikova NI, Novikova NB, Roshal OD, Vashenko OV, Lipson VV (2014) (16*E*)-16-Pyrazolilmethylen-17-oxosteroids of androstene and estran series and chiral-nematic liquid-crystal mixtures on their base. UA Patent 10,665,7
20. Dehaen W, Mashentseva AA, Seitembetov TS (2011) Allobetulin and its derivatives: synthesis and biological activity. Molecules 16:2443–2466
21. Babak NL, Gella IM, Semenenko AN, Shishkina SV, Shishkin OV, Musatov VI, Lipson VV (2014) α, β-Unsaturated ketones based on allobetulone. Russ J Org Chem 50:1048–1055
22. Krasutsky PA., Karlson RM., Karim R (2002) Triterpenes having human antifungal and antiyeast activity. US Patent 01,282,10A,1
23. De Gennes PG (1974) The physics of liquid crystals. Oxford University Press, Oxford
24. Kutulya LA, Semenkova GP, Yarmolenko SN, Fedoryako AP, Novikova IE, Patsenker LD (1993) New chiral imines based on s-alpha-phenylamines and s-alpha-benzylethylamines in induced cholesteric and smectic mesophases. 1. structure and twisting ability of chiral additives in induced cholesteric mesophases of 4-alkyl-4′-cyanobiphenyls. Kristallografiya 38:183–191
25. Sheldrick GM (2008) A short history of SHELX. Acta Crystallogr Sect A A64:112–122
26. Zefirov NS, Palyulin VA, Dashevskaya EE (1990) Stereochemical studies. Quantitative description of the ring puckering via torsional angles. The case of six-membered rings. J Phys Org Chem 3:147–158
27. Bader RFW (1990) Atoms in molecules. A quantum theory. Clarendon, Oxford
28. Espinosa E, Molins E, Lecomte C (1998) Hydrogen bond strengths revealed by topological analyses of experimentally observed electron densities. Chem Phys Lett 285:170
29. Walsh AD (1949) The structures of ethylene oxide, cyclopropane and related molecules. Trans Faraday Soc 45:179–190
30. Burgi H-B, Dunitz JD (1994) Structure correlation 2. VCH, Weinheim, pp 741–784